

NEARBY GROUPS OF GALAXIES. I. THE NGC 1023 GROUP

R. BRENT TULLY

Institute for Astronomy, University of Hawaii
 Received 1979 July 27; accepted 1979 October 19

ABSTRACT

New H I radial velocities of galaxies have been acquired in a large region around NGC 1023. Hierarchical clustering techniques have been developed as a means to describe the clustering properties of galaxies. The most satisfactory method merges entities sequentially on the basis of a maximization of the gravitational force. Plotted as a function of the luminous density, the hierarchy provides a direct estimate of the mass-to-light ratio that is required if any given level is to be gravitationally bound. The hierarchy can be used as a guide toward the delineation of groups that have physical significance. Arguments based on crossing times and application of the virial theorem lead to the identification of a group of 13 galaxies in the region around NGC 1023 which is almost certainly bound. It is argued that the superposed galaxy UGC 2080 = IC 239 is, in fact, located in the background. The mass derived by a dynamical analysis is consistent, within the uncertainties, with the sum of the masses associated with the disks of the individual galaxies. The derived virial-mass-to-light ratio is $19(+28, -14) M_{\odot}/L_{\odot}$ ($H_0 = 75 \text{ km s}^{-1} \text{ Mpc}^{-1}$). However, this mass might be underestimated since, according to the gravitational clustering theory, the group is near its maximum extent today and one expects most of the binding energy to be in the form of potential energy. A means of establishing a lower limit for the cosmological density parameter is discussed. There are two small groups each roughly 5 Mpc from the NGC 1023 group, and their integrity has not been jeopardized by the tidal shear created by the NGC 1023 group since, at least, the epoch $z \sim 3$.

Subject headings: galaxies: clusters of — galaxies: individual — galaxies: redshifts

I. INTRODUCTION

The total mass associated with galaxies or groups of galaxies is a parameter of fundamental importance to cosmology. The kinematics of individual galaxies cannot be studied sufficiently far from their centers that we can be confident we are observing all of the mass. In addition, there may be intracluster material. The best estimates of the total mass in the universe that is clumped like galaxies will come from interpretations of the kinematics of groups and clusters.

For the great clusters, it has been appreciated for quite some time from application of the virial theorem that mass-to-luminosity ratios must be quite high. Our present concern is with the situation in small groups of galaxies. Lately there has been active debate on this topic (Rood, Rothman, and Turnrose 1970; Materne and Tammann 1974; Turner and Sargent 1974; Gott and Turner 1977; Rood and Dickel 1978). It has been possible for conclusions to range from mass-to-luminosity ratios not substantially different from values normally associated with individual galaxies ($M_{VT}/L_B \sim 10$) to ratios that are beyond an order of magnitude higher ($M_{VT}/L_B \sim 300$). Very likely, the greatest uncertainty in most of these studies has been in the detailed definition of group membership. Our principal contribution will be to provide a large body of new and accurate redshifts. These data are allowing us to identify groups with greater clarity than previously possible.

In spite of this optimistic statement, the description of galaxies in terms of groups is often ambiguous. In

this first paper of a series, we are concentrating on one specific group which has the merit of being isolated. In this regard it should not at all be considered typical and we will not attempt to generalize on the conclusions drawn from this one example. It just seemed desirable to begin with a simple case. A similar reasoning must have motivated the earlier investigation of this same group by Materne (1974).

II. A GENERAL DESCRIPTION OF THE REGION

Excluding members of the Local Group, there are 36 galaxies in the region $120^\circ < l < 170^\circ$ and $-50^\circ < b < 0^\circ$ with measured (corrected) systemic velocities less than 1500 km s^{-1} . Table 1 provides basic data describing these galaxies, and Figure 1 illustrates their projected distribution on the sky. The paucity of galaxies north of latitude -15° must be attributed to obscuration within the Milky Way.

There is an evident clustering of galaxies in the vicinity of $l = 144^\circ$ and $b = -20^\circ$ which has been referred to for a long time as the NGC 1023 group (cf. Humason, Mayall, and Sandage 1956). Figure 2 illustrates properties of the distribution of galaxies with respect to the center of mass of this clustering (determined further on). Plotted along the abscissa are systemic velocities with respect to the barycentric velocity of the group. Plotted along the ordinate are the squares of the projected separations from the group center of mass, so that horizontal bands on the figure represent equal areas on the sky.

It is clear from Figure 2 that 13 galaxies are closely

TABLE 1
BASIC DATA

Designation	l (deg)	b (deg)	τ^a	a_H^b (arcmin)	r_H^b	$B_r^{0,i,c}$ (mag)	v_i^d (km s $^{-1}$)	$\sigma(v_i)^e$ (km s $^{-1}$)	Alternate Names
NGC 278...	123.06	-15.32	3	4.2	1.00	10.88	883	9	...
NGC 404...	127.05	-27.01	-2	5.5	1.00	10.74	178	18	...
UGC 731...	126.13	-13.15	10	3.7	0.92	13.02	874	10	DDO 9
UGC 891...	134.26	-49.80	9	4.7	0.52	13.09	784	10	DDO 10
NGC 628...	138.62	-45.70	5	12.0	1.00	9.62	797	10	M74
UGC 1176...	139.74	-45.37	10	6.8	0.82	12.70	769	10	DDO 13
UGC 1195...	141.25	-47.08	10	5.0	0.38	12.47	893	15	...
NGC 660...	141.60	-47.36	1	9.8	0.45	10.97	980	10	...
0140+19...	139.23	-41.24	10	4.5	0.32	13.66	647	12	...
UGC 1249...	137.96	-33.90	9	10.2	0.33	11.17	506	20	VV 338=IC 1727
NGC 672...	138.01	-33.78	6	11.3	0.36	10.52	591	20	VV 338
UGC 1281...	136.89	-28.71	8	6.5	0.28	11.42	343	10	...
NGC 746...	135.12	-16.37	10	3.4	0.75	12.43	913	12	...
NGC 784...	140.91	-31.60	8	9.7	0.27	11.04	362	10	...
UGC 1561...	143.45	-35.75	10	2.5	0.70	14.12	739	10	V ZW 173
UGC 1807...	139.98	-17.12	10	3.8	1.00	12.74	814	10	...
NGC 891...	140.37	-17.43	3	15.0	0.25	9.33	711	10	...
UGC 1865...	143.35	-23.10	9	5.0	0.82	13.06	741	12	DDO 19
NGC 925...	144.89	-25.16	7	14.0	0.61	10.07	709	10	...
NGC 949...	144.06	-21.62	7	5.2	0.67	11.99	773	10	...
NGC 959...	145.08	-22.99	9	3.9	0.61	12.33	766	10	...
UGC 2014...	143.79	-20.04	10	3.7	0.58	13.72	736	10	DDO 22
UGC 2017...	148.32	-28.99	10	3.8	0.82	13.96	1154	10	...
UGC 2023...	146.19	-24.73	10	4.4	0.94	12.75	762	10	DDO 25
UGC 2034...	143.15	-18.28	10	5.0	0.87	12.35	751	10	DDO 24
UGC 2053...	148.23	-28.01	10	3.5	0.60	13.51	1169	10	DDO 26
UGC 2080...	144.33	-19.50	6	6.5	0.97	11.46	1071	10	IC 239
UGC 2082...	150.89	-31.68	5	8.3	0.25	11.34	832	10	...
NGC 1003...	144.00	-17.54	6	7.7	0.45	11.17	793	10	...
NGC 1012...	149.08	-27.19	11	4.7	0.56	12.37	1120	10	...
NGC 1023...	145.03	-19.08	-2	11.6	0.37	9.14	776	33 ^f	ARP 135
NGC 1036...	155.52	-36.58	13	2.6	0.72	13.29	889	12 ^f	MARK 370
NGC 1058...	146.37	-20.38	5	6.0	1.00	11.71	675	10	...
UGC 2259...	147.15	-19.79	8	4.2	0.80	12.89	741	15	...
NGC 1156...	156.32	-29.20	10	5.9	1.00	11.98	477	6 ^f	...
UGC 2684...	166.33	-32.74	10	3.1	0.54	14.50	417	10	...

^a Morphological type. The nomenclature is from the *Second Reference Catalogue* (de Vaucouleurs *et al.* 1976).

^b Holmberg dimension. Adjustments from other systems follow Paturel (1975) for major diameters, a_H , and Fisher and Tully (1975) for the ratio of minor to major diameters, r_H .

^c Blue magnitudes corrected for galactic absorption, A_b , and absorption as a function of inclination in the external galaxy, A_i . The uncorrected magnitudes are in the *Second Reference Catalogue* system. The corrections (Fisher and Tully 1980) are given by $A_b = -0.15 + 0.21/\sin |b|$; $A_i = -0.3[\ln(e^{-\sec i} + 0.01) + 1]$.

^d Systemic velocities, adjusted for solar motion of 300 km s $^{-1}$ toward $l = 90^\circ$, $b = 0^\circ$.

^e Estimated measurement errors in velocities.

^f Optical velocities; all others are H I measurements by Fisher and Tully (1980).

associated both on the plane of the sky and in velocity. One galaxy, UGC 2080 = IC 239, is closely associated on the plane of the sky but is significantly removed in velocity. The location of this one galaxy will have a substantial effect on our analysis.

The correlation of the width of the neutral hydrogen-line profile with absolute magnitude (Tully and Fisher 1977) can be exploited to determine redshift-independent distances for those spiral galaxies which are not too face-on or disturbed. The method can be applied to five of the 13 galaxies closely associated with NGC 1023 and three of the remaining 23 galaxies. The results are summarized in Table 2. With the group barycentric velocity 751 ± 16 km s $^{-1}$ and the distance modulus 30.0 ± 0.3 mag, the corresponding value for the Hubble constant is 75 ± 11 km s $^{-1}$ Mpc $^{-1}$. This value is in agreement with our earlier results and we will use it to determine distances to galaxies in the

field. However, this scale assumes the "old" Hyades distance and it may be desirable to augment all distances by 10%. The galaxy UGC 2082 is located at roughly the same distance as the NGC 1023 group and the pair NGC 784 and UGC 1281 are at half the distance. These results are consistent with the respective redshifts. It must be cautioned that there are more than normal uncertainties in these distances because these galaxies are at low galactic latitudes.

III. HIERARCHICAL CLUSTERING METHODS

a) The Methods

There have been two philosophies applied to the identification of groups. On the one hand, there has been the subjective approach (cf. de Vaucouleurs 1975) which does not anticipate what properties a group may have in a quantitative sense but simply

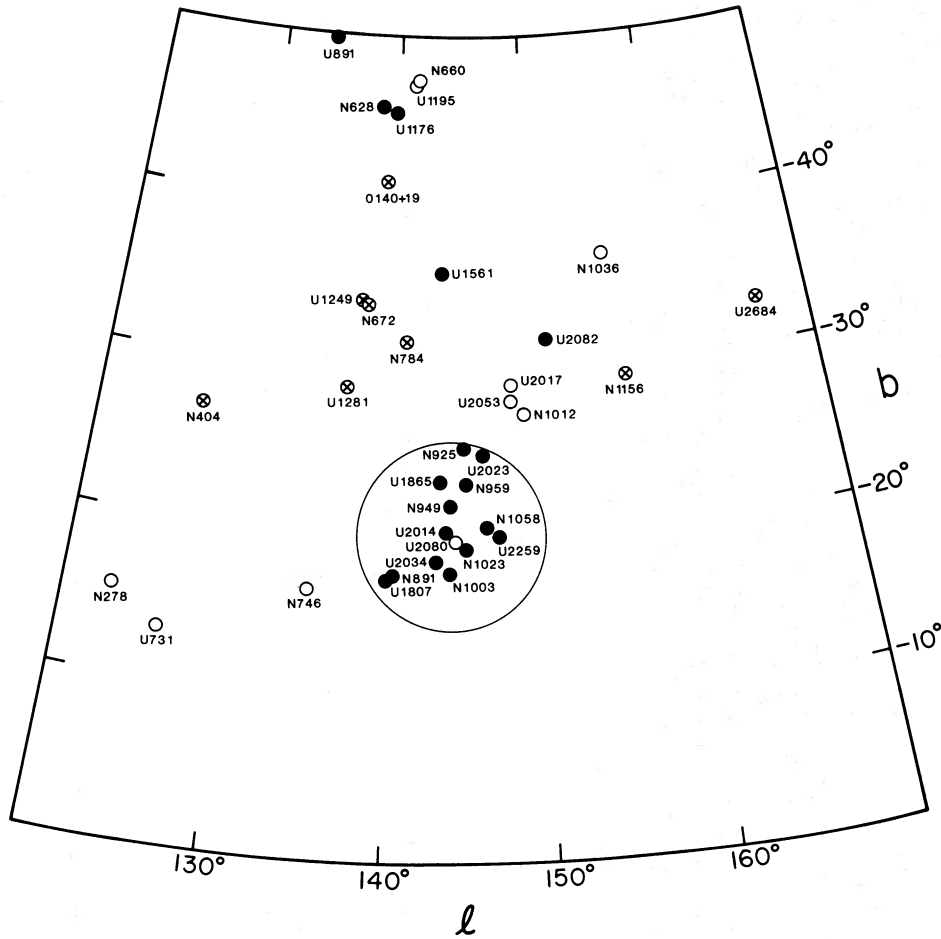


FIG. 1.—Distribution on the sky of the 36 galaxies with $v_i < 1500 \text{ km s}^{-1}$ in the area around NGC 1023. Filled circles represent those galaxies with systemic velocities within 3σ of the barycentric velocity of the proposed group. Open circles represent galaxies redshifted with respect to these constraints, and circles with crosses represent galaxies which are blueshifted. The proposed NGC 1023 group is enclosed by a large circle with a radius of $1.5R_\Omega$.

TABLE 2
DISTANCES

Designation	i^a (deg)	ΔV_{20}^b (km s^{-1})	$\Delta V_{20}^{i,b}$ (km s^{-1})	$B_T^{o,i,c}$ (mag)	$M_B^{o,i,c}$ (mag)	μ_0^d (mag)	D^d (Mpc)
NGC 891.....	81	495	501	9.33	-20.39	29.72	8.8
NGC 925.....	54	224	277	10.07	-18.92	28.99	6.3
NGC 949.....	49	196	260	11.99	-18.76	30.75	14.2
NGC 1003.....	66	235	257	11.17	-18.73	29.90	9.6
NGC 959.....	54	180	222	12.33	-18.37	30.70	13.8
Average.....						30.01 ± 0.33	
Surrounding area							
UGC 2082.....	81	222	225	11.34	-18.40	29.74	8.9
UGC 1281.....	78	144	147	11.42	-17.35	28.77	5.7
NGC 784.....	79	124	126	11.04	-16.96	28.00	4.0

^a Inclination.

^b Observed H I profile width at 20% of full intensity and profile width corrected for projection effects.

^c Blue magnitudes from Table 1 and absolute magnitudes from magnitude—H I profile width relationship.

^d Distance moduli and distances.

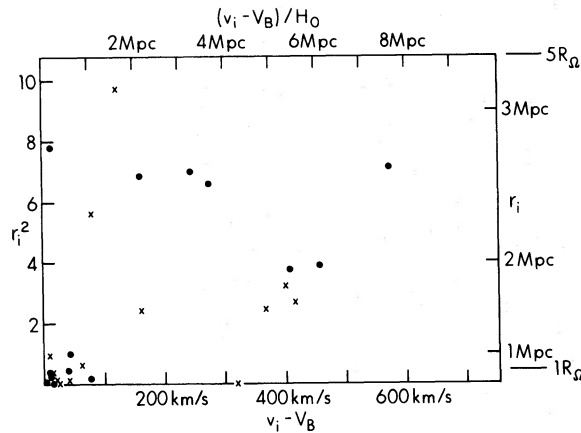


FIG. 2.—Separation of individual galaxies in velocity and in projection from the center of the NGC 1023 group. Velocity differences are given along the abscissa, with objects redshifted with respect to the barycentric velocity denoted by crosses and objects which are blueshifted denoted by dots. The squared projected separations with respect to the group center of mass are given along the ordinate. The vertical scales and the scale across the top of the figure presume $H_0 = 75 \text{ km s}^{-1} \text{ Mpc}^{-1}$. The 13 galaxies most definitely associated with the NGC 1023 group are those which are clustered near zero separation in the lower left corner.

asks that the group stand out (spatially, in velocity, by type, in luminosity) from the background of galaxies that are reasonably uniformly distributed. As a rule, this method is probably successful in identifying the quintessence of groups and it is successful over a wide range of conditions, from compact clusters to very loose configurations. However, the method can suffer from very subtle biases.

On the other hand, there have been attempts to develop completely objective algorithms that would assure reproducibility. For example, Turner and Gott (1976) identify all regions in which the number density on the sky of galaxies drawn from a magnitude-limited catalog exceeds a certain factor times the mean density. It is acknowledged that such methods frequently accredit groups with systems which are actually separated in the line of sight and any attempts to distinguish such cases have, once again, been subjective. Also, it is difficult to define an algorithm which is flexible enough to pick out the full range of clustering conditions.

We are trying to develop a quantitative approach which leads to group identifications consistent with our subjective perceptions. To this end, we have explored variants of the hierarchical clustering techniques first applied to this problem by Materne (1978). Suppose there are N galaxies initially considered to be separate entities. At each step in the development of the hierarchy, those two entities that optimize some specified parameter (such as minimum separation) are merged. After $N - 1$ steps, there will be only one entity comprised of all N galaxies. It might be perceived that there is a level in the hierarchical procedure which separates real groups from the background.

Materne specified that each successive merger should satisfy the Ward criterion which requires that, with a

measure of the dispersion in separations within an entity, the *increase* in this measure be a minimum. The line-of-sight separations are inferred from redshifts but the relative scale of the projected and line-of-sight dimensions remains a free parameter.

Materne plotted the ensuing hierarchy as a function of the total dispersion in all the clusters and in all dimensions. A disadvantage of this procedure is that, at a given merger, this function will contain contributions which were introduced by earlier, completely unrelated mergers. The value of the function at a merger between two specific entities is dependent on the size of the sample. As a slight variant, one could plot the hierarchy as a function of the *incrementation* in this function with each merger. However, the Ward method has a further disadvantage. Because the function which measures the dispersion in separations increases with the number of galaxies which join an entity, there is a preference that the entities be kept small. Consequently, it may arise that an isolated galaxy at a distance from a cluster is merged in preference to an entity with several members which is situated closer.

The only other application of a similar procedure was by Paturel (1979), who actually went in the opposite sense of dismemberment. Unfortunately, he chose to apply his procedures to the region around the Virgo cluster where the use of velocities as a measure of line-of-sight separations is especially treacherous.

We have tried two approaches. The simplest is the method of centroid clustering that Materne has already discussed. At each merger, we select the two entities which have the minimum separation between their centers of mass. As Materne has done, we use redshift to provide the third dimension but we retain a free parameter to describe the coupling between projected and line-of-sight distances. Materne has criticized the centroid clustering method because reversals may occur, that is, the minimum distance between two entities may decrease as the consequence of a merger. The criticism is that the hierarchy has no meaningful interpretation in the face of reversals, even though Materne has already cautioned us to consider hierarchical clustering as only a mathematical tool. Reversals are small in amplitude and serve to remind us not to take the details too seriously.

Our computational procedures are an extension of the program given by Anderberg (1973). Equating luminosity with mass, we determined center-of-mass separations from the update algorithm:

$$r_{tj}^2 = \frac{L_p}{L_p + L_q} r_{pj}^2 + \frac{L_q}{L_p + L_q} r_{qj}^2 - \frac{L_p L_q}{(L_p + L_q)^2} r_{pq}^2, \quad (1)$$

where the current merger is between p and q which are separated by a distance r_{pq} and have luminosities L_p and L_q , the merged entity will be called t , and it is necessary to determine the separation r_{tj} of t from all entities j given knowledge of r_{pj} and r_{qj} .

The application of the method requires some

assumptions about the luminosity weights and the coupling between projected and line-of-sight distances. All members of a group should have the same distance modulus irrespective of redshift, yet foreground and background galaxies will have distance moduli correlated with redshift. If the characteristic crossing time within a group is comparable to the age of the universe, then line-of-sight distances derived assuming a uniform Hubble flow will be statistically correct; but if the crossing time is substantially less, then *within*, the gravitational domain of the group, such an assumption would give line-of-sight distances which are too large. Our procedure has been to make extreme assumptions, on the proposition that configurations that persist are likely to be real; then to iterate to the most self-consistent description. Specific results in the region of the NGC 1023 group will be discussed after we introduce our second method to describe the clustering.

The problem with the simple centroid method is that it is not very physical. Two dwarf galaxies 1 Mpc apart would merge at the same instant as the Virgo cluster and a galaxy 1 Mpc from its core. The physical parameter is not the separation but the gravitational *force* between pairs. In our second method, we derive a quantity which is related to the inverse of this force, F_{ij} :

$$\frac{1}{F_{ij}} \propto \frac{r_{ij}^2}{L_{\max}}, \quad (2)$$

where L_{\max} is the larger of L_i and L_j , and r_{ij}^2 has been derived with equation (1). We then merge those pairs for which this quantity is a minimum. It is now possible to get substantial reversals since, with mergers between two massive (luminous) groups, the divisor, L_{\max} , in equation (2) can increase sharply. Also, the "contrast" between a group and the field will be diminished since separations are being divided by an ever increasing number. Nevertheless, a much more physical *sequence* of mergers takes place.

While force is the proper measure for merging, a preferred measure for a judgment of the reality of an entity is the *density*. Consequently, while we merge following the minimization of $1/F_{ij}$, we plot the subsequent hierarchy as a function of the inverse of the luminous density, l_{ij} :

$$\frac{1}{l_{ij}} = \frac{4\pi r_{ij}^3}{L_{\max}}. \quad (3)$$

The critical density for closure, ρ_c , is approximately given by

$$\rho_c = l(M/L)_c, \quad (4)$$

which is to say that if the luminous density of an entity is l then for that entity to be bound the mass-to-light ratio must exceed $(M/L)_c$. If one is so bold as to assume a value for $(M/L)_c$ then a horizontal cut in the hierarchy plotted as a function of $1/l$ separates bound and unbound clusters. We prefer to use the hierarchy simply to identify prospective groups as input for the more detailed analysis of § IV.

b) Application in the Region around NGC 1023

The hierarchy developed using the centroid method is shown in Figure 3 (NGC 404, which has been proposed as a member of the Local Group, has been excluded from this and the subsequent figure as, in all tests, it is easily the last galaxy to join the hierarchy). Here, luminosities were derived assuming a Hubble flow, except that all 13 galaxies most closely associated with NGC 1023 were taken to be at the same distance. There was no substantial difference between this case and the case in which luminosities were derived assuming a constant distance modulus to all candidates.

In Figure 3 we have presumed that there is no deviation from the Hubble flow in deriving line-of-sight distances. The effect of altering this assumption can be important since we are plotting the hierarchy as a function of the *square* of the distance between entities. However, even with the assumption that line-of-sight separations are only half that expected from the Hubble flow, there are only modest alterations. NGC 672 and UGC 1249 couple more tightly, NGC 660 and UGC 1195 couple more tightly to each other and to the triplet around NGC 628, and the quartet NGC 1012, UGC 2017, UGC 2053, and UGC 2080 is coupled more tightly to the NGC 1023 group. However, this latter merger still does not occur until a squared separation of 6.1 on a centroid hierarchy diagram. One must assume a departure of a factor of 3 from the Hubble expansion for UGC 2080 = IC 239 to couple to the NGC 1023 group in preference to the NGC 1012 triplet. We conclude that it takes a large departure from the Hubble flow to merge UGC 2080 to the NGC 1023 group and that in all other respects the centroid hierarchy is quite stable.

The hierarchy developed using the force method is shown in Figure 4. Again, luminosities were derived assuming a Hubble flow, except for the 13 galaxies most certainly associated with the NGC 1023 group. Variations in luminosity through the assumed distance moduli have larger effects now, but the differences are still insubstantial. If we were to take the same distance modulus for all galaxies in deriving intrinsic luminosities, then the merger between NGC 1012 and the pair UGC 2017 and UGC 2053 would be lost because of the relative decrease in their luminosities, but a merger would occur between NGC 784 and UGC 1281 because their relative luminosities would increase.

If we assume, once again, that line-of-sight separations are only half the value expected from the Hubble flow, the alterations to the hierarchy in Figure 4 are still minor. The order in which some isolated galaxies append to the NGC 1023 group changes, with NGC 746, UGC 2080 = IC 239, NGC 784, UGC 1281, and the triplet NGC 1012, UGC 2017, and UGC 2053 joining sooner. The group around NGC 628 is significantly tightened and, in fact, unites with NGC 660 and 0140+19 before joining with NGC 1023. NGC 672 and UGC 1249 merge. Once more, we conclude that the hierarchy is qualitatively stable. There are much larger variations between the hierarchies

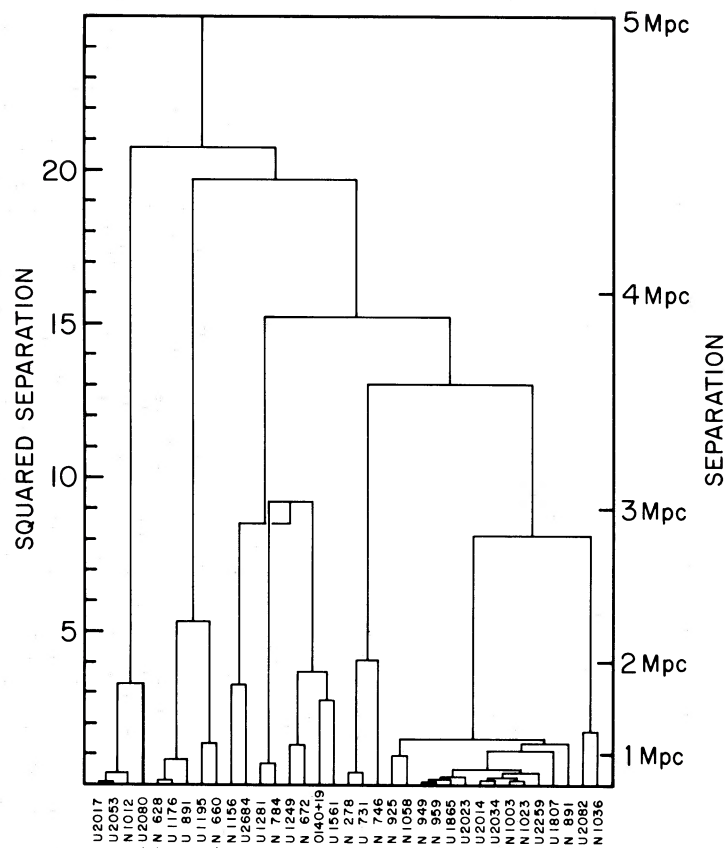


FIG. 3.—Centroid hierarchy. The sequence of mergers is plotted as a function of the square of the separation between the centers of mass of previously merged entities. The first merger involving the most controversial system, UGC 2080 = IC 239, is emphasized by a thicker line. The seven most luminous systems are identified by asterisks.

displayed in Figures 3 and 4 than there are within the variants of one of the methods.

Intercomparing the hierarchies derived by the two different methods, the most obvious *similarity* is the delineation of a cleanly separated group of 13 galaxies which includes NGC 1023. The most obvious *difference* is that there is a lot more subclustering in the centroid hierarchy. Only the few massive galaxies are effective as subcluster cores with the force method. Pairs of galaxies at several virial radii from the NGC 1023 group might merge in Figure 3 because they are marginally closer to each other than to the group, but they clearly could not be bound in such a tidal field. Figure 4 provides a more realistic description. The only advantage to pursuing the centroid method is that it does not demand the assumption of a fixed relationship between mass and luminosity and might reveal the existence of structure in instances where there are large departures from “normal” values of this ratio.

Let us devote some attention to Figure 4. As an aside, the most luminous galaxies have been identified along the abscissa and it may be noted that the most substantial reversals occur in the step after a merger involving these systems. By chance, two of the last three galaxies merged to the core of the NGC 1023

group were among the more luminous members of the group. As a further aside, we have provided a scale alongside luminosity in Figure 4 which roughly indicates the required value of the mass-to-light ratio if the closure density is to be realized at each level of the hierarchy.

Figure 4 tells us that in this considerable volume of space there are only three merger cores other than the NGC 1023 group. The non-Hubble flow case suggested that there is a fourth: the NGC 672 pair. In § IV we will investigate whether these small entities might be bound from a consideration of their internal kinematics. Here, we check to see if the proximity of NGC 1023 would *permit* them to be bound, in the spirit of the analysis of groups in the vicinity of the Virgo cluster by Hartwick (1976). Assuming spherical symmetry, a uniform Hubble flow, and a constant mass-to-light ratio, the Roche limit R_G of a small group will be

$$R_G \leq \left(\frac{L_G}{4L} \right)^{1/3} \frac{R}{1+z}, \quad (5)$$

where the summed luminosities of the galaxies within the small group and the NGC 1023 group are, respectively, L_G and L ; the separation of the group from NGC 1023 is R ; and the galaxies were formed at a

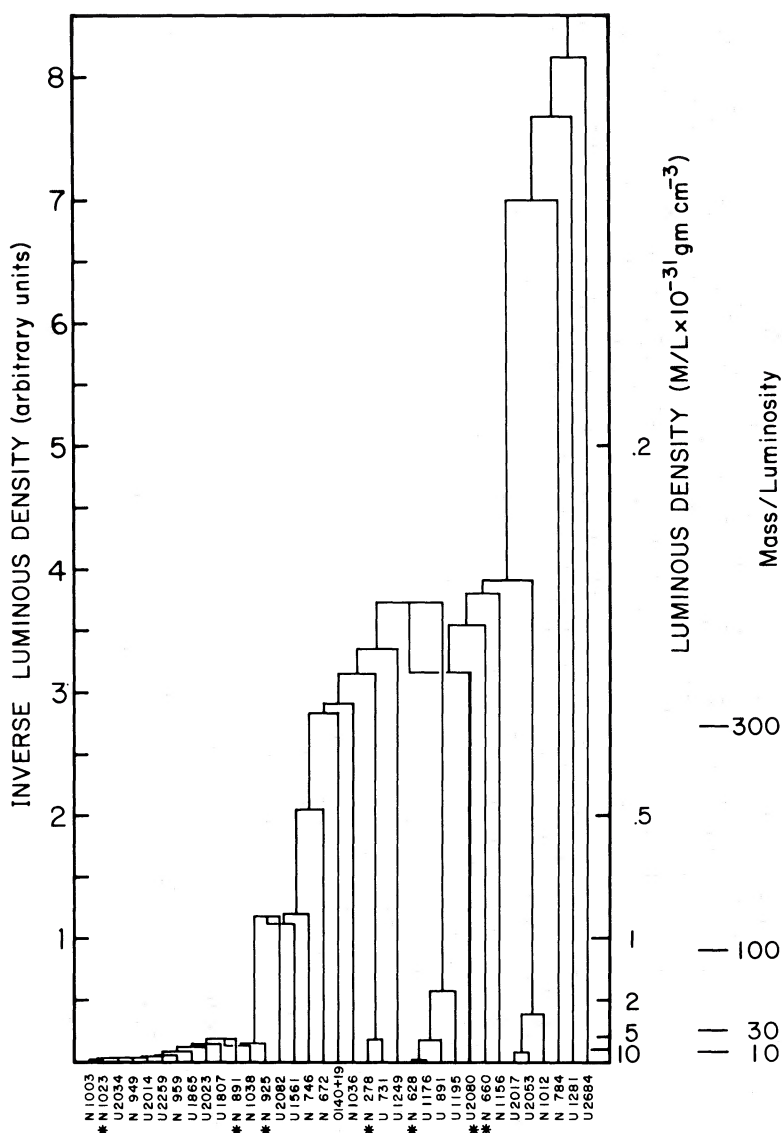


FIG. 4.—Force hierarchy. The sequence of mergers is plotted as a function of the inverse mass (luminosity) density. The extreme right-hand vertical scale indicates the mass-to-light ratio that would be required at each level if the hierarchy is to be gravitationally bound. Again, the first merger involving UGC 2080 is emphasized and the seven dominant galaxies are identified.

redshift z . If for R_G we substitute the virial radius that we determine for these groups in §IV, then we can derive a value for the redshift such that if the groups were formed at any more recent epoch then they could be stable. The assumption is made that the separate groups are expanding freely with the universe, and this is likely to have been true only while the cosmological density parameter Ω has been less than unity. Our results are summarized in Table 3. The NGC 278 pair is very unlikely to be bound, while the NGC 672 pair would never have suffered outside influences were it always at the present separation. More interestingly, the only entities larger than pairs could have been stable back to z of 1.5 to 3. We will find that if the NGC 1012 triplet is stable then the mass-to-light ratio must be large, and while NGC 628 may be a bound triplet

or quartet it is not likely to retain NGC 660, so only tentative conclusions about the epoch of the formation of groups can be drawn. However, it is comforting to find that there are no gross violations of the tidal disruption test in the form of small, bound groups in close proximity to the larger NGC 1023 group.

Perhaps more interesting is the limit to the epoch of cluster formation (in a freely expanding universe) established by a consideration of the effect of tidal shear caused by galaxies in the field on the NGC 1023 group itself. Within the limited volume under consideration, the dominant interaction is with the NGC 628 group (although it is possible that the dominant interaction is actually with a cluster outside the sample). Again, equation (5) achieves equality with $z \sim 3$. It is argued below that the NGC 1023 group is

TABLE 3
TIDAL EFFECT OF NGC 1023 GROUP ON OUTLYING GROUPS

Group	No. Galaxies	l_{cm}^a (deg)	b_{cm}^a (deg)	V_B^b (km s ⁻¹)	R^c (Mpc)	R_Ω^d (Mpc)	L_G^e (L_\odot)	z_{max}^f
NGC 1023.....	13	144.0	-19.7	751	...	1.03	9.7×10^{10}	2.8 ^g
NGC 628.....	5	138.5	-46.0	844	4.7	0.56	4.1×10^{10}	3.0
NGC 1012.....	3	148.8	-27.7	1130	5.3	0.53	0.63×10^{10}	1.5
NGC 278.....	2	123.4	-15.1	882	3.9	1.2	1.1×10^{10}	0
NGC 672.....	2	138.0	-33.8	567	3.6	0.025	0.86×10^{10}	39

^a Center of mass coordinates.

^b Group barycentric velocities.

^c Distance from the NGC 1023 group.

^d Statistically deprojected virial radii.

^e Sum of the luminosities of the galaxies in each group.

^f Redshift corresponding to equality condition in eq. (5).

^g Earlier than this limit, the NGC 1023 group would have been disrupted by the tidal effect of the NGC 628 group.

almost certainly bound, so this result must be considered significant.

IV. VIRIAL AND CROSSING TIME ANALYSIS

Particularly because of the dangers involved in coupling the line-of-sight and plane-of-sky dimensions, it would be imprudent to apply a rigid interpretation of either of the hierarchies that have been derived. Materne (1979) has emphasized this point. He has proposed an algorithm for the evaluation of the likelihood of group membership which he calls a probability density function. If the spatial and velocity distributions of groups can be given a functional description, then the probability of the occurrence of a given deviation, either in velocity or in separation on the plane of the sky, can be compared with the probability of the occurrence of a field galaxy. The method offers the obvious advantages that it is objective and takes into account both the velocity and spatial domains. It does suffer the operational disadvantages that assumptions are required concerning the choices of the functional descriptions and the distribution of field galaxies.

We will follow a slightly different tack. Guided by the hierarchies illustrated in Figures 3 and 4, and by those others derived with different assumptions regarding deviations from the Hubble expansion, we consider the consequences of all configurations that plausibly constitute bound groups. In somewhat the spirit of Materne's analysis, the probabilities of very deviant velocities or positions are derived assuming functional dependencies. Other factors are also considered, including crossing times, the implications to a virial theorem analysis, and, to a lesser degree, the more subjective implications of the morphology of certain galaxies in this sample. The results of eight cases regarding the composition of the NGC 1023 group are summarized in Tables 4 and 5. Certain of these cases deserve some discussion.

a) Cases 1 and 2

There can be little doubt that the 13 galaxies that are closely associated in projection and velocity in Figure 2 and stand apart in each of the hierarchies are

members of a common group. For all of these systems, in any plausible analysis, $r_\theta < 1.6R_\Omega$ and $|v_i - V_B| < 3V_p$ (terms defined in notes to Table 4).

In case 1, it was assumed that the ratio of the mass to luminosity in the lenticular NGC 1023 to the mass to luminosity in the remaining (spiral and irregular) galaxies is 2:1. In case 2, this ratio is taken to be unity. The barycentric velocity is affected by these choices, but little else is. In particular, there is little effect on the derived virial mass. Tests with more extreme variations of mass to luminosity as a function of type demonstrate that the virial mass is stable to 10%. We have a slight preference for the results of case 1 over those of case 2 because in the former instance the distribution of velocities is quite symmetrical about the barycentric velocity.

In each of these cases, the probable projected velocity dispersion is an amazingly low 30 km s⁻¹. As a consequence, the crossing time is roughly equal to the age of the universe. Equivalently, there is no difference between the tangential and radial group dimensions when a uniform Hubble expansion is assumed and statistical deprojection corrections are applied:

$$\langle \log 2r_v / (4/\pi)r_\theta \rangle = -0.06 \pm 0.15.$$

This result places the applicability of the virial theorem in doubt. The uncertainties in the analysis are discussed in § V. Note that the result $\langle 2r_v \rangle \sim \langle 4r_\theta/\pi \rangle$ provides a justification for our preferred hierarchical models which assume a uniform Hubble flow.

b) Cases 3 and 4

In the past, the spiral galaxy UGC 2080 = IC 239 has inevitably been considered a member of the group (de Vaucouleurs 1975; Sandage and Tammann 1975) because it is a prominent galaxy and is quite centrally located in the group on the plane of the sky. However, until recently a radial velocity was not available for UGC 2080. We will argue that this galaxy is *not* a member of the group.

i) The velocity of this galaxy deviates from the group barycentric velocity by 310 km s⁻¹. In terms of the now much increased group dispersion (increased

TABLE 4
 VIRIAL ANALYSIS FOR EIGHT CASES: GROUP PARAMETERS

Case	Constituents	No.	V_B^a (km s ⁻¹)	V^b (km s ⁻¹)	V_p^b (km s ⁻¹)	R_G^c (Mpc)	R_I^d (Mpc)	$T_I H_0^e$	M_{VTI}/L_B^f	$\sigma(M/L)^g$
1.....	"certain" $M/L(E:S) = 2:1$	13	751 ± 16	34	29 ± 9	0.66	0.52	0.96	19	± 12
2.....	"certain" $M/L(E:S) = 1:1$	13	743 ± 16	35	31 ± 9	0.66	0.59	1.01	19	± 11
3.....	"certain" plus U2080	14	761 ± 17	64	62 ± 5	0.56	0.51	0.44	67	± 11
4.....	case 3 plus N1012 trio	17	769 ± 17	82	81 ± 4	0.58	0.56	0.37	115	± 12
5.....	"certain", plus N746	14	754 ± 16	38	34 ± 8	0.67	0.55	0.86	25	± 11
6.....	case 5 plus U1561, U2082	16	756 ± 15	40	36 ± 7	0.72	0.70	1.03	28	± 11
7.....	case 6 plus 3 "possible"	19	733 ± 24	77	75 ± 6	0.73	1.10	0.78	98	± 16
8.....	all within $5R_G$, $V_0 < 1500$ (except N404)	26	726 ± 29	138	137 ± 4	0.74	1.19	0.46	271	± 16

NOTE.—Throughout the table, italics are used to emphasize deviant values.

^a Barycentric velocity.

^b Observed and probable velocity dispersion in the line of sight (Materne 1974).

^c Projected virial radius.

$$R_G = \sum_{\text{pairs}} m_i m_j / \left(\sum_{\text{pairs}} m_i m_j / r_{ij} \right)^{1/2}$$

^d Projected inertial radius (Jackson 1975)

$$R_I = \left(\sum_i m_i r_i^2 / \sum_i m_i \right)^{1/2}$$

^e Crossing time as a function of the age of the universe; $T_I H_0 = R_I H_0 / (2)^{1/2} V_p$.

^f Virial mass to blue luminosity ratio. Potential and kinetic energies have been calculated following Materne (1974).

^g Uncertainties in mass-to-light estimate associated with uncertainties in measured velocities only (Rood and Dickel 1976).

TABLE 5
VIRIAL MASS ANALYSIS FOR EIGHT CASES: INDIVIDUAL GALAXY PARAMETERS

CASE AND NAME	$M_B^{0.1a}$	$v_l - V_B^b$	$\log (r_v/r_\theta)^c$	r_θ/R_G^d	$T_\theta H_0^e$	FRACTIONS ^f			KE/Mass ^g
						Mass	PE	KE	
1 ("certain")									
N 1023.....	-20.9	+24	+0.21	0.31	0.38	0.52	0.38	0.21	0.4
N 891.....	-20.7	-41	-0.11	1.05	1.31	0.22	0.21	0.34	1.5
N 925.....	-19.9	-43	-0.24	1.51	1.89	0.11	0.092	0.19	1.7
N 1003.....	-18.8	+41	+0.20	0.53	0.66	0.040	0.090	0.063	1.6
N 1058.....	-18.3	-77	+0.37	0.66	0.82	0.024	0.053	0.16	6.6
N 949.....	-18.0	+21	-0.11	0.56	0.70	0.018	0.033	0.001	0.1
N 959.....	-17.7	+14	-0.52	0.96	1.21	0.013	0.020	0.000	0.0
U 2034.....	-17.7	-1	-1.52	0.38	0.48	0.013	0.032	0.000	0.0
U 1807.....	-17.3	+62	+0.03	1.18	1.48	0.009	0.031	0.039	4.4
U 2023.....	-17.3	+10	-0.85	1.49	1.86	0.009	0.012	0.000	0.0
U 2259.....	-17.1	-11	0.81	0.81	1.02	0.008	0.016	0.000	0.0
U 1865.....	-16.9	-11	-0.65	0.96	1.20	0.007	0.009	0.000	0.0
U 2014.....	-16.3	-16	+0.35	0.14	0.18	0.003	0.010	0.000	0.0
3 ("certain" plus)									
U 2080.....	-18.5	+310	+1.79	0.12	0.06	0.029	0.11	0.75	26
4 (case 3 plus)									
N 1012.....	-17.6	+351	+0.48	2.64	1.05	0.012	0.007	0.24	19
U 2053.....	-16.5	+400	+0.52	2.74	1.08	0.004	0.002	0.11	24
U 2017.....	-16.0	+385	+0.47	3.02	1.20	0.002	0.001	0.066	23
5 ("certain" plus)									
N 746.....	-17.6	+159	+0.14	2.29	2.51	0.012	0.008	0.27	23
6 (case 5 plus)									
U 2082.....	-18.7	+76	-0.36	3.19	3.54	0.032	0.014	0.12	3.9
U 1561.....	-15.9	-17	-1.08	3.78	4.20	0.002	0.000	0.000	0.0
7 (case 6 plus)									
N 672.....	-19.5	-142	-0.14	3.58	1.93	0.061	0.11	0.22	3.5
U 1249.....	-18.8	-227	+0.06	3.61	1.94	0.034	0.10	0.31	9.1
N 1156.....	-18.0	-256	+0.12	3.51	1.89	0.016	0.006	0.19	11.7
8 (all in cases 4 and 7 plus)									
N 784.....	-19.0	-364	+0.35	2.90	0.86	0.034	0.018	0.24	7.0
U 1281.....	-18.6	-383	+0.42	2.63	0.78	0.024	0.012	0.19	7.8
U 731.....	-17.0	+148	-0.20	4.23	1.26	0.005	0.001	0.006	1.1

NOTE.—Throughout the table, italics are used to emphasize deviant values.
^a Absolute blue magnitudes corrected for absorption as indicated in Table 1 and assuming a distance of 10.0 Mpc.
^b Individual systemic velocity minus the group barycentric velocity.
^c Ratio of line-of-sight to plane-of-sky separations,

$$\frac{r_v}{r_\theta} = \frac{(v_l - V_B)/H_0}{D \sin \theta_i}$$

where D is the distance to the group and θ_i is the angle an individual galaxy subtends from the center of mass.
^d Ratio of the plane-of-sky separation to the projected virial radius of the group.
^e Individual crossing time. $T_\theta = (4/\pi)r_\theta/3^{1/2}V_p$.
^f The fractions of mass, potential energy, and kinetic energy associated with the individual galaxy.
^g Ratio of the kinetic energy fraction to the mass fraction.

from 29–31 to 62 km s⁻¹!) this represents a deviation of 5.0 σ . However, this larger group dispersion may not be meaningful given that the second-largest deviation in a sample of 14 is only 1.3 σ . As an alternative estimate of the group dispersion, a Gaussian was least-squares fitted to a velocity histogram of the 14 galaxies. A standard dispersion of 43(+12, -10) km s⁻¹ was determined. Conservatively taking the dispersion to be 55 km s⁻¹, we find that the velocity associated with UGC 2080 represents a 5.6 σ deviation. A chi-squared test reveals that the probability of such an occurrence is 5×10^{-3} .

ii) If UGC 2080 were a member of the group, then this one galaxy with 3% of the total mass would have 75% of the kinetic energy. The kinetic-energy fraction to mass fraction ratio is 26, whereas the largest value for this ratio in case 1 or case 2 was 6.6.

iii) If UGC 2080 were assumed to be a member of the group then one of two unlikely dynamical situations would be implied. On the one hand, there could be the large mass suggested by the case 3 virial analysis, but then there would be a large deviation from a normal distribution in velocities in the sense that most velocities would be unexpectedly low. On the other hand, the group mass might be in line with the estimates of cases 1 and 2 and UGC 2080 might have received a large peculiar motion as the consequence of a multibody interaction. It is unlikely that this impetus would have been received from NGC 1023 alone (at a projected separation of 150 kpc, the radial velocity difference between these two is 25% greater than the velocity of escape from NGC 1023) and the two other massive systems, NGC 891 and NGC 925, are 10¹⁰ years removed in terms of the group dispersion. While there are aspects of the morphology of NGC 1023 that are peculiar, none of the other principal members of the group, including UGC 2080, have characteristics suggestive of tidal effects.

iv) *In retrospect*, the morphology of UGC 2080 suggests that it is in the background. From its spiral structure we would guess this galaxy to be intrinsically more luminous than NGC 925, even though in apparent dimensions and luminosity it is smaller and fainter.

v) The centroid hierarchy associates UGC 2080 with a group including NGC 1012, UGC 2017, and UGC 2053. All four of these galaxies have similar velocities ($V_p = 34$ km s⁻¹), but UGC 2080 is sufficiently removed on the plane of the sky that it would have been tidally sheared from the others by the proximity of the NGC 1023 group. The NGC 1012 triplet can have survived as a group only if its members are well removed from NGC 1023, as their redshifts would imply.

vi) Given a random distribution of the galaxies in the sample not associated with the NGC 1023 group then, statistically, 1.3 galaxies unassociated with the group would lie within the circle of $1.5R_\Omega$ radius shown in Figure 1.

c) Cases 5 and 6

The situation regarding NGC 746 is the most ambiguous, and we treat it as case 5. The velocity

difference of 159 km s⁻¹ represents a 4.7 σ departure from the group mean, and the chi-squared probability of this occurrence with a normal distribution and 14 systems is 0.08. The fractional projected distance $r_\theta/R_\Omega = 2.3$ represents a 2.5 σ departure from the mean, and the probability of this occurrence, now with only one degree of freedom, is 0.01. Consequently, if velocity and projected separation are viewed as independent, then the combined probability that they both deviate so substantially is about 10⁻³. Alternatively, if we follow Materne (1979) and add the spatial and velocity departures from the means in quadrature then, with 14 degrees of freedom, the chi-squared probability is 10⁻². The crossing time $T_\theta H_0 = 2.5$ strongly suggests that the galaxy is not bound to the group. If it were bound and virialized, this galaxy with 1% of the total observed mass would possess 21% of the kinetic energy. Even so, the formal value of the virial-mass-to-light ratio in case 5 is only 30% higher than those in cases 1 and 2.

The two additional small galaxies considered in case 6, UGC 2082 and UGC 1561, are even less likely to be bound on projected separation and crossing time arguments; but assuming they were, they would only affect the virial-mass-to-luminosity ratio by 10%.

d) Cases 7 and 8

The three additional galaxies in case 7 were suggested as possible group members by de Vaucouleurs (1975). Case 8 includes all galaxies in the sample within $5R_\Omega$ except the possible Local Group system NGC 404. For these implausible configurations the virial mass estimates are much larger but not beyond the range of values found in the literature for other groups.

e) The Probability Density Function

The method that Materne (1979) has proposed can be approximated, although because our sample is not magnitude-limited the term describing the background density of galaxies must be modified. It is evident that not all possible configurations need be tested, that only four galaxies in addition to the "certain" 13 have any plausibility as members of the NGC 1023 group. We find the candidacies of UGC 2080 and NGC 746 to be strongly rejected (probabilities of 10⁻⁸ and 3×10^{-3} , respectively). The candidacies of UGC 2082 and UGC 1561 are marginally accepted (probabilities of 0.7 and 0.6, respectively), although the results for the latter two are sensitive to assumptions regarding the distribution of field galaxies.

f) Outlying Groups

Data for the only other plausible groups in the volume of space under discussion are presented in Table 6. For complementary reasons, the two pairs need not be seriously considered. The members of the NGC 278 pair have a projected separation of 760 kpc so there is little compulsion to suppose they are bound and the members of the NGC 672 pair have a separation of only 16 kpc, which is not likely to be typical of the past.

TABLE 6
VIRIAL MASS ANALYSIS FOR FOUR OUTLYING GROUPS

Group	No.	V_B (km s ⁻¹)	V^a (km s ⁻¹)	V_p^a (km s ⁻¹)	R_Ω^a (Mpc)	R_I^a (Mpc)	$T_I H_0$	M_{VT}/L_B	$\sigma(M L)^b$
N 1012.....	3	1136 ± 13	21	20 ± 4	0.34	0.19	0.52	88	± 39
+ U 2080...	4	1097 ± 18	35	34 ± 4	<i>1.24</i>	<i>1.18</i>	<i>1.86</i>	<i>347</i>	± 75
N 628.....	4	801 ± 7	24	24 ± 4	0.32	0.22	0.48	45	± 15
+ N 660....	5	836 ± 39	75	74 ± 4	0.36	0.27	0.20	<i>214</i>	± 25
N 672.....	2	561 ± 28	41	38 ± 10	0.02	0.01	0.01	14	± 7
N 278.....	2	882 ± 1	3	0 ± 12	0.76	0.25	<i>13</i>	0	...

NOTE.—Italics throughout the table emphasize deviant values.

^a Projected velocities and dimensions.

^b Errors associated with uncertainties in measured velocities only.

The triplet around NGC 1012 has the properties of a bound group, with the group dispersion only $V_p = 20 \text{ km s}^{-1}$, the virial radius $R_\Omega = 340 \text{ kpc}$, and the crossing time $T_I = 0.5H_0^{-1}$. The virial-mass-to-light ratio is rather large ($M_{VT}/L = 88 M_\odot/L_\odot$) in spite of the low velocity dispersion because all three systems are small: at 15 Mpc the largest galaxy NGC 1012 has $M_B^{0,i} = -18.5 \text{ mag}$. UGC 2080 has a very similar redshift to these three but it is 2.4 Mpc removed in projection, and we have already argued that it could not be bound with the others because of the gravitational effect of the NGC 1023 group.

The situation in the region around NGC 628 is not very clear. If NGC 660 is bound with NGC 628, then an order of magnitude more mass than that associated with the disks of galaxies must be located in the group. If it is not bound, then there is little evidence for more mass than found in disks, especially if UGC 1195 is coupled with NGC 660 rather than NGC 628. There are other galaxies in the vicinity, such as 0140+19, which the force hierarchy suggests are under the tidal influence of the NGC 1023 group. The situation suggests a scenario in which, at earlier epochs, only those configurations of galaxies most tightly bound could escape disruption as a result of the proximity of the NGC 1023 group. Galaxies such as NGC 660 and 0140+19 may be examples of systems released to the field.

V. UNCERTAINTIES IN THE VIRIAL MASS

In case 1, we derived a value for the characteristic crossing time of $T_I = 0.96H_0^{-1}$. Alternative methods have been used to estimate the crossing times following Gott and Turner (1977), and the average velocity and radius crossing time introduced by Rood and Dickel (1978). The extreme values over both case 1 and case 2 are $0.7 < TH_0 < 1.0$. The applicability of the virial theorem is in considerable doubt.

Nonetheless if, for the moment, the pertinence of the virial theorem is accepted and membership is restricted to the "certain" 13 galaxies, then it is possible to estimate the uncertainty in the virial mass estimate. Rood and Dickel (1979) have examined this matter in detail, and, for the most part, we follow their analysis. The dominant errors are in velocity measurements, velocity projection corrections, luminosity

corrections, and distance uncertainties. The possible error associated with velocity measurements is dominated by the lower quality of the velocity for NGC 1023 itself. Regarding projection corrections, although the kinetic energy term in the virial analysis is dominated by the contributions of three massive systems we can have some confidence that we are not victims of a very unlikely projection circumstance because the unweighted dispersion of these three ($36 \pm 6 \text{ km s}^{-1}$) is consistent with the unweighted group mean ($29 \pm 6 \text{ km s}^{-1}$). The uncertainties assigned to luminosities and distances account only for random errors and not for the systematic effects associated with the choice of absorption correction algorithms or the distance scale.

All errors except for those in the observed velocities should be combined logarithmically. The summation is given in Table 7. The virial-mass-to-luminosity ratio (13 "certain" members only) is

$$M_{VT}/L_B = 19(+19, -14)M_\odot/L_\odot.$$

There remains the finite possibility that NGC 746 is a member, and if this is accepted as a constraint on the errors, then

$$M_{VT}/L_B = 19(+28, -14)M_\odot/L_\odot.$$

The corresponding mass for the group is $2 \times 10^{12} M_\odot$.

With a value for the mass of the cluster from the virial theorem and the observed dimensions it is possible to estimate the phase that is being observed in the process of cluster formation, assuming there is no dissipation in this process. The time scale for collapse is given by Gunn and Gott (1972):

$$T_c = 1.6 \times 10^{11} (R_\Omega^3/M_{12})^{1/2} \text{ years}, \quad (6)$$

where the mass M_{12} is in units of $10^{12} M_\odot$, the radius is in Mpc, and account is taken in the constant of a transformation from a harmonic mean radius to a projected virial radius. Assuming $R_\Omega = 0.66 \text{ Mpc}$ and $M_{12} = 2$, then the cluster is expected to be in the virialized regime when $t_{vir} \geq \frac{3}{2}T_c \sim 9 \times 10^{10} \text{ years}$.

It must be concluded that the group is still at an early phase in the collapse. In fact, it must be rather near its maximum extent. At the moment collapse begins, $t_{max} = \frac{1}{2}T_c$ and $R_\Omega^{max} \sim 2R_\Omega^{virialized}$. So,

TABLE 7
SOURCES OF ERROR OTHER THAN OBSERVED VELOCITIES

Source of Error	σ (log M_{VT}/L_B)
Projection.....	0.18
Orbits.....	0.04
Relative M/L	0.06
Luminosities ^a	0.12
Distances ^a	0.11
Quadrature summation.....	0.25

^a Possible systematic errors.

assuming the dimension to insert in equation (6) is half the observed dimension, $t_{\max} \sim 1.1 \times 10^{10}$ years.

There are two conclusions that can be drawn. In the first place, since most of the binding energy is expected to be in the form of potential energy, the virial mass will probably be an underestimate of the true mass. However, it cannot be an underestimate by an order of magnitude or the collapse time would be lower to a degree that the cluster would be approaching the virialized regime.

In the second place, it might be possible to set a lower limit on the cosmological density parameter Ω on the proposition that the onset of cluster formation could not be occurring today in a very open universe. In an open universe, density fluctuations would have grown via gravitational instability since the epoch of recombination, $1 + z_{\text{rec}} \sim 10^3$, until $1 + z \sim \Omega^{-1}$ as $\delta\rho/\rho \sim (1 + z)^{-1}$ and subsequently remained constant (cf. Gott 1977). If $\delta\rho/\rho$ had not grown roughly to unity by the time the universe began to expand freely at $1 + z \sim \Omega^{-1}$, then the fluctuations will never collapse. Gunn and Gott (1972) provide a relationship between the amplitude of density fluctuations at recombination and the collapse time:

$$\left(\frac{\delta\rho}{\rho}\right)_{\text{rec}} \approx \left(\frac{\pi}{H_0 T_c}\right)^{2/3} \Omega^{-1/3} (1 + z_{\text{rec}})^{-1}. \quad (7)$$

The density enhancement at $1 + z = \Omega^{-1}$ is then:

$$\left(\frac{\delta\rho}{\rho}\right)_{\Omega^{-1}} \approx \left(\frac{\pi\Omega}{H_0 T_c}\right)^{2/3}. \quad (8)$$

With $T_c \sim 2 \times 10^{11}$ years and $H_0 = 75 \text{ km s}^{-1} \text{ Mpc}^{-1}$, the condition $(\delta\rho/\rho)_{\Omega^{-1}} \geq 1$ implies $\Omega \geq 0.5$. The dependence on Ω is sufficiently weak that if $\Omega \sim 0.1$ then $(\delta\rho/\rho)_{\Omega^{-1}} \sim 0.35$, which may be only marginally different from unity. However, the mean density of the universe cannot be much smaller if the gravitational instability model is to be reconciled with the collapse time scale associated with the NGC 1023 group.

VI. CONCLUSIONS

We reject the possibility that UGC 2080 = IC 239 is a member of the NGC 1023 group on the grounds that such a large velocity deviation in a normal distribution has a very low probability, that if the galaxy were included then there is no evident dynamical situation that is plausible, that a luminosity classification would suggest the system is in the background,

and that if it is at the distance implied by its redshift then it would not be alone.

The possibility that NGC 746 is a member is negligibly small, although the possibility is conceded in order to provide a conservative constraint on the errors associated with the estimate of the mass of the group. The two galaxies that have similar velocities to those in the group but are removed in projection, UGC 1561 and UGC 2082, were allowed as members by the probability density function. However, from a consideration of crossing times it seems unlikely that either of them could be carrying kinetic energy out of the group and so warrant inclusion in a dynamical analysis. There are no additional galaxies with unmeasured redshifts that could substantially affect the analysis: within $3R_\Omega$ all galaxies brighter than $B_T^0 = 12.0 \text{ mag}$ ($M_B^0 = -18.0 \text{ mag}$ at 10 Mpc) have measured redshifts. An attempt was made to observe all galaxies brighter than $B_T^0 = 13.5 \text{ mag}$. UGC 2069 is the only good candidate that remains undetected, and if it were a member it would possess only 1% of the observed mass in the group.

We can summarize the constraints on the mass of the group. On the low side, our results are consistent with the hypothesis that there is no additional mass to that normally associated with the disks of galaxies. It is likely that the group is at least bound, although there is no compelling argument for this on the basis of crossing times. Roberts's (1969) mean value of the ratio of mass to light for spiral galaxies is $\langle M/L_B \rangle = 7 M_\odot/L_\odot$ in our system of luminosities and distances. On the basis of this value and with the case 1 assumption that the lenticular NGC 1023 has twice the mass-to-light fraction of the spirals and irregulars, then $\text{KE}/|\text{PE}| = 1.0$ for the group. By comparison, Dickel and Rood (1978) obtained a significantly larger $\langle M/L_B \rangle = 23 M_\odot/L_\odot$ for spirals (in our system) by choosing mass models employing flatter rotation curves and larger characteristic turnover radii, and their value suggests $\text{KE}/|\text{PE}| = 0.3$. Consequently, there is almost certainly sufficient mass to satisfy the criterion that the group be bound: $\text{KE} + \text{PE} < 0$. Our conclusions in this respect are substantially in agreement with Materne's (1974).

On the high-mass side, the formal error in the virial-mass analysis, accepting NGC 746 as a member, sets the limit: $M_{VT}/L_B < 47 M_\odot/L_\odot$. However, if the group has not collapsed significantly then this upper limit is quite uncertain. If many small groups are at a similar phase in their collapse, this fact may explain the large range of M_{VT}/L_B that is observed (Rood and Dickel 1979).

On the assumption that structure in the universe has evolved in the fashion described by the gravitational clustering theory, and given the consequent conclusion that the group about NGC 1023 is just now in limbo between expansion and collapse, then the universe cannot be extremely empty. A rough limit $\Omega > 0.5$ is established. Evidently, a result based on a single group is not to be given much weight.

In the volume we have sampled (8 Mpc on a side and 20 Mpc deep), there are only two other groups larger than pairs. Each of these is sufficiently removed

from the NGC 1023 group that they would not have been threatened with tidal disruption, nor the NGC 1023 group by them, since $z \sim 3$. If these groups did form more recently than $z \sim 3$, there is the implication that $\Omega \gtrsim 0.25$. This argument is independent of the one above. It will be important to carry out this group disruption test in more densely populated regions as a probe of the epoch of cluster formation.

In conclusion, the force hierarchy provides an attractive method of delineating groups. Spheres of gravitational influence are easily visualized. We have not yet attempted to establish quantitative criteria for the selection of groups through the hierarchy because we have not yet explored a sufficient range of group conditions. The NGC 1023 area was chosen for an initial test of the method because it is more straightforward than some other regions.

This discussion would not have been possible without the support of Richard Fisher. He was responsible for all the neutral hydrogen observations that are presented in this paper. The referee drew attention to the recent and important contribution by Materne. This research was sponsored by NSF grant AST 76-12159.

Note added in manuscript, 1979 October.—Hart, Davies, and Johnson (1980) have recently claimed that the unusual neutral hydrogen profile in the direction of NGC 1023 is caused by the superposition of an H I cloud centered 14' northeast of the galaxy and redshifted by 275 km s^{-1} . They propose that the H I cloud is at a common distance with UGC 2080 and that both are to the background of the NGC 1023 group, which is a position consistent with our own. Our dynamical argument that UGC 2080 be excluded from the group is strengthened by this discovery, because it is difficult to admit that there would be *two* objects associated with the group which differ in radial velocity by only 24 km s^{-1} between themselves but deviate from the group mean by 300 km s^{-1} .

If we accept the radial velocity and error for NGC 1023 given by Hart, Davies, and Johnson ($769 \pm 12 \text{ km s}^{-1}$), then the conclusions drawn from a virial analysis are essentially unchanged, except that the uncertainty associated with velocity measurements becomes almost negligible. With the case 1 sample,

$$M_{VT}/L_B = 20(+16, -10) M_{\odot}/L_{\odot}.$$

The upper limit to the mass in the group, derived with the assumption that NGC 746 is a member of the group, remains unchanged.

REFERENCES

- Anderberg, M. R. 1973, *Cluster Analysis for Applications* (New York: Academic).
- de Vaucouleurs, G. 1975, *Stars and Stellar Systems*, vol. 9, ed. A. Sandage, M. Sandage, and J. Kristian (Chicago: University of Chicago Press), p. 557.
- de Vaucouleurs, G., de Vaucouleurs, A., and Corwin, H. G. 1976, *Second Reference Catalogue of Bright Galaxies* (Austin: University of Texas Press).
- Dickel, J. R., and Rood, H. J. 1978, *Ap. J.*, **223**, 391.
- Fisher, J. R., and Tully, R. B. 1975, *Astr. Ap.*, **44**, 151.
- . 1980, *Atlas and Catalog of Nearby Galaxies*, in preparation.
- Gott, J. R. 1977, *Ann. Rev. Astr. Ap.*, **15**, 235.
- Gott, J. R., and Turner, E. L. 1977, *Ap. J.*, **213**, 309.
- Gunn, J. E., and Gott, J. R. 1972, *Ap. J.*, **176**, 1.
- Hart, L., Davies, R. D., and Johnson, S. C. 1980, *M.N.R.A.S.*, submitted.
- Hartwick, F. D. A. 1976, *Ap. J. (Letters)*, **208**, L13.
- Humason, M. L., Mayall, N. U., and Sandage, A. R. 1956, *A.J.*, **61**, 97.
- Jackson, J. C. 1975, *M.N.R.A.S.*, **173**, 41P.
- Materne, J. 1974, *Astr. Ap.*, **33**, 451.
- . 1978, *Astr. Ap.*, **63**, 401.
- . 1979, *Astr. Ap.*, **74**, 235.
- Materne, J., and Tammann, G. A. 1974, *Astr. Ap.*, **37**, 383.
- Paturel, G. 1975, *Astr. Ap.*, **40**, 133.
- . 1979, *Astr. Ap.*, **71**, 106.
- Roberts, M. S. 1969, *A.J.*, **74**, 859.
- Rood, H. J., and Dickel, J. R. 1976, *Ap. J.*, **205**, 346.
- . 1978, *Ap. J.*, **224**, 724.
- . 1979, *Ap. J.*, **233**, 418.
- Rood, H. J., Rothman, V. C. A., and Turnrose, B. E. 1970, *Ap. J.*, **162**, 411.
- Sandage, A. R., and Tammann, G. A. 1975, *Ap. J.*, **196**, 313.
- Tully, R. B., and Fisher, J. R. 1977, *Astr. Ap.*, **54**, 661.
- Turner, E. L., and Gott, J. R. 1976, *Ap. J. Suppl.*, **32**, 409.
- Turner, E. L., and Sargent, W. L. W. 1974, *Ap. J.*, **194**, 587.

R. BRENT TULLY: Institute for Astronomy, 2680 Woodlawn Drive, Honolulu, HI 96822